

H.J. Tobias<sup>1)</sup>, G.L. Sacks<sup>2)</sup>, Y. Zhang<sup>1)</sup>, J.T. Brenna<sup>1)</sup>

## **Progress towards comprehensive 2d gas chromatography combustion isotope ratio mass spectrometry (GCxGCC-IRMS)**

<sup>1)</sup>Division of Nutritional Sciences, Cornell University, Ithaca NY USA

<sup>2)</sup>Department of Food Science & Technology, Cornell University, Ithaca NY USA

### *Abstract*

We report the very first coupling of Comprehensive Two-dimensional Gas Chromatography (GCxGC) to on-line Combustion Isotope Ratio Mass Spectrometry (C-IRMS). An optimized low dead volume combustion interface between the GCxGC, containing a longitudinal cryogenic modulator, and an IRMS facilitated the “fast GC” peakshapes required for GCxGC separation in a second GC column (GC2). For this work, a fused silica capillary with no film was used for GC2 in order to evaluate minimal peak widths attainable with the steroids investigated. When not modulated, the steroids had full width at half maximum (FWHM) peak widths increase over a very large range (2866-6777ms) as compound GC1 retention times increased (720-1130s). However, when modulated at 4 sec intervals, the FWHM sliced peak widths of the steroids do not vary and fall in the range of 288-384ms. A mixture of four steroids was analyzed for the <sup>13</sup>C isotopic composition of each component when not modulated and when modulated at 4 sec intervals. Preliminary data on the integration of sliced peaks resulted in average standard deviations of 0.6 ‰ (0.35-1.23) and accuracies within 0.4 ‰ (0.19-0.72). These results indicate the feasibility of using GCxGC separations with on-line C-IRMS as advanced methodology for synthetic steroid detection in doping.

### *Introduction*

Carbon isotope ratio (CIR) testing is currently an accepted and powerful tool for detecting synthetic steroids used in doping, most notably testosterone, and has been described extensively in the literature (Aguilera *et al.* 1999). This is based on kinetic isotope effects in biological systems, where the CIR of synthetic testosterone is different from that of

naturally produced testosterone due to a difference in source carbon. Therefore, the use of exogenous testosterone in doping can be detected by measuring the CIR of an endogenous reference steroid in the precursor pathway to testosterone, along with either testosterone itself or its metabolites.

High precision gas isotope ratio mass spectrometry (IRMS), the established technique for determination of the fractionation of stable isotopes, requires the chemical transformation of a sample into a gas representative of its isotopic makeup (Asche *et al.* 2003). In synthetic steroid detection, compound specific isotopic analysis (CSIA) of  $^{13}\text{C}/^{12}\text{C}$  isotope ratios is conducted by gas chromatography combustion IRMS (GCC-IRMS). Using this method, GC effluent is chemically converted to  $\text{CO}_2$  gas via an on-line metal oxide combustion micro-reactor, and the relative abundance of the isotopomers of the  $\text{CO}_2$  gas,  $^{12}\text{CO}_2$ ,  $^{13}\text{CO}_2$ , and  $^{16}\text{CO}_2$  ( $m/z$  44, 45, 46, respectively) are measured via IRMS to determine the CIR of the individual steroids. The CIR is reported in  $\delta$  notation with respect to an international standard, in units of per mil (‰). The CIR is expressed as  $\delta^{13}\text{C}_{\text{VPDB}} = (\text{R}_{\text{SPL}} - \text{R}_{\text{VPDB}})/(\text{R}_{\text{VPDB}}) \times 1000$ , where  $\text{R}_{\text{SPL}}$  is the CIR of the sample and  $\text{R}_{\text{VPDB}}$  is the CIR of the international standard Vienna PeeDee Belemnite ( $\text{R}_{\text{VPDB}}=0.0112372$ ).

Traditional GC (1DGC) has insufficient resolution to separate many components in complex mixtures such as urinary steroid extracts. Comprehensive two dimensional gas chromatography (GCxGC) is more suitable for advanced non-targeted testing methodology for synthetic steroids when coupled with IRMS. GCxGC was first developed by Liu and Phillips in the early 1990's (Liu and Phillips 1991), with variations and improvements developed since then (Marriott and Kinghorn 1997; Mondello *et al.* 2008). GCxGC employs two chromatographic columns with orthogonal properties operating in tandem. The use of a modulator, utilizing cryogenics, between the first and second columns allows a plug of eluting components from the first column to be trapped and continuously transferred onto the second column in 2-10 sec intervals, generating a secondary chromatogram at each 2-10 sec point in the primary chromatogram. Usually, the first column is a long conventional capillary column that separates components in 30-60 min, while the second column is short and operated very rapidly achieving fast isothermal or approximately isothermal separation within each interval. GCxGC has been successfully used to separate and classify hundreds of chemical species in many different types of complex mixtures such as petroleum, ambient air, and lipid samples. The major advantages of GCxGC over 1DGC include enhanced non-targeted component resolving power (up to x10), the formation of chemically similar

compound patterns in the 2D contour chromatogram, and enhanced sensitivity through solute band re-concentration onto the second GC column (up to x10).

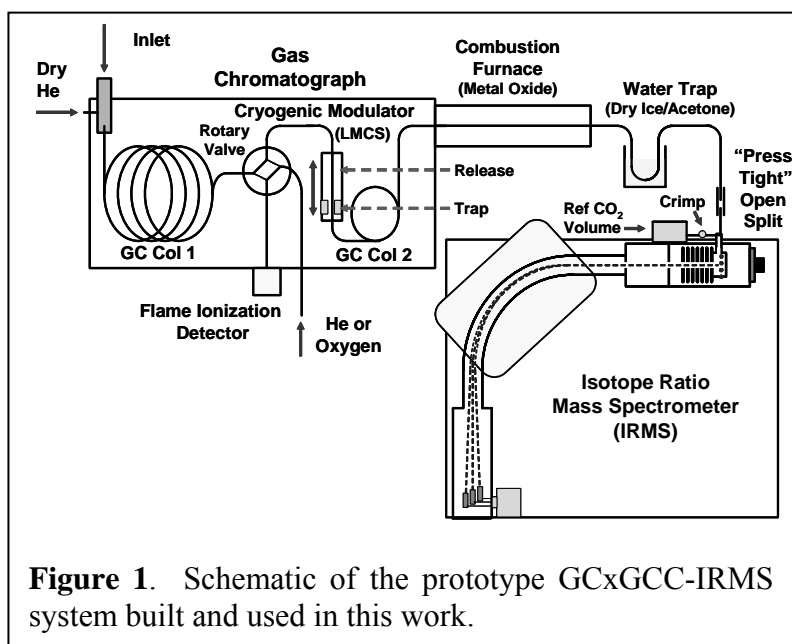
The full width at half maximum (FWHM) peak widths that result from GCxGC are on the order of 10's to 100's of milliseconds; while the FWHM peak widths from 1DGC are on the order of seconds. Due to this, the detector used to analyze the GCxGC effluent requires a duty cycle of at least 25Hz or greater. The preservation of the fast GC peaks generated from GC2 separation through an on-line combustion interface and the efficient detection of those peaks are significant considerations for the coupling of IRMS to GCxGC. Such an endeavor is non-trivial and wrought with many complications. In previous work developing fast GCC-IRMS (Sacks *et al.* 2007), critical components were evaluated for minimizing peak broadening effects in the GC and combustion interface. The main theme of the optimizations involved reducing GC effluent pathway dimensions, dead volumes, and connections. These concepts were exploited here for the development of GCxGCC-IRMS. Here, we report the construction of a prototype GCxGCC-IRMS system and demonstrate the feasibility of using GCxGC separations for advanced compound specific stable isotope measurements of steroids for CIR tests in sport doping.

### *Materials and Methods*

Chemicals and Standards. The steroids 5 $\alpha$ -androstan-3 $\beta$ -ol acetate (5 $\alpha$ -andro-AC), 5 $\alpha$ -androstan-3 $\alpha$ -ol-17-one acetate (andro-AC), 5 $\beta$ -androstan-3 $\alpha$ -ol-11,17-dione acetate (11-keto-AC), and 5 $\alpha$ -cholestane (cholestane) were acquired from Steraloids (Newport, RI, USA) and used without further purification. The steroid mixture analyzed for this work was prepared in 2-propanol at a concentration of 100 ng/ $\mu$ l. These steroids were previously calibrated relative to the NIST natural gas reference material RM 8559 (>80% methane of coal origin) to determine their  $\delta^{13}\text{C}_{\text{VPDB}}$ , and is described in detail elsewhere (Zhang *et al.* 2008).

GCxGCC-IRMS system. The schematic of the GCxGCC-IRMS system is depicted in Figure 1. An HP6890A gas chromatograph (Agilent Technologies, Menlo Park, CA) was interfaced to a MAT 252 IRMS (Finnigan, Bremen, Germany). A Longitudinal Modulation Cryogenic System developed by Marriott *et al.* (Marriott and Kinghorn 1997) (LMCS, Chromatography Concepts, Sandringham, Australia) was installed between GC column 1 (GC1), and GC column 2 (GC2). GC1 and GC2 were held in the same GC oven at the same temperature. When peak modulation was performed, the LMCS was cooled to -20°C using liquid CO<sub>2</sub> at 9

min and actuated at 10 min. A split/splitless inlet was used for sample introduction. On-line conversion of analyte effluent to carbon dioxide gas was accomplished using a narrow inner diameter capillary combustion reactor operated at 925°C to retain sharp GC2 peak shapes. The combustion reactor comprised of a 0.45m x 0.25mm i.d. x 0.36mm o.d. deactivated fused silica



capillary containing one oxidized 0.19m x 0.10mm diameter Cu/Mn/Ni wire and one 0.19m x 0.10mm diameter Pt wire. A rotary valve (VICI, Houston TX) was used for solvent diversion in order to prevent premature depletion of combustion reactor metal oxide.

A 1 m long deactivated fused silica capillary with a 0.10 mm i.d. was used as a transfer capillary between the combustion reaction and the open split. Water vapor generated from the combustion process was removed from the system before the IRMS by immersing 10 cm of the transfer capillary into a dry/ice acetone water trap at -78°C. Press-tight fittings (Restek, Bellafonte PA) were used for connections between GC1, GC2, and the combustion reactor. A portion of the dry effluent was sampled into the IRMS through a press tight fitting open split and 1 m x 0.075 mm i.d. capillary that was fitted at the inlet to the IRMS.

GC Parameters for Analysis of Steroid Mix. The steroid mix contained an approximately equal mass mixture of 5 $\alpha$ -andro-AC, andro-AC, 11-keto-AC, and cholestane. A volume of 1  $\mu$ l of 100 ng/ $\mu$ l solution was injected for non-modulated analysis at a 40:1 split for signal size comparison and 10:1 split for quantitative analysis, while 1  $\mu$ l was injected for 4 sec modulated analysis at a 40:1 split in all analyses. GC1 was a 30 m x 0.25 mm i.d. x 0.25  $\mu$ m film DB5 (J&W Scientific, Agilent Technologies, Menlo Park CA) and GC2 was a 1 m x 0.10 mm i.d. fused silica capillary with no film. The head pressure was set to 28 psi @ 80°C with a flow rate of 1.2 ml/min in constant flow mode. The GC oven was initially held at 80°C for 1 min, ramped at 30°C/min to 270°C, where it was held for 18 min, and then ramped

at 10°C/min to 300°C, where it was held for 1 min.

Data Acquisition. SAXICAB, a home-built LabVIEW-based IRMS data acquisition and reduction system, was used to monitor the  $m/z$  44, 45, and 46 data streams from the MAT 252 head amplifiers using three 24-bit National Instruments NI4351 digitizers (Austin, TX). The data was collected at 50 Hz, but consecutive points were averaged to halve the size of files, resulting in an effective data acquisition rate of 25 Hz. The standard RC (resistance-capacitance) time constant of the  $m/z$  46 faraday cup detector was reduced by exchanging the resistor in order to prevent broadening of fast GC2 peaks for the  $m/z$  46 signal, as described previously (Sacks *et al.* 2007). The standard configuration was changed from  $R (1e11 \Omega) \times C (2 \text{ pF}) = \tau (200 \text{ ms})$  to  $R (3e10 \Omega) \times C (2 \text{ pF}) = \tau (60 \text{ ms})$ .

Data Processing. All data sets were processed for quantitative isotopic analysis through SAXICAB using the individual summation method with an individual background definition. Also, a minor modification to the conventional time correction was applied due to fast GC2 peaks, detailed previously (Sacks *et al.* 2007). The contribution of  $^{17}\text{O}$  to the  $^{45}\text{CO}_2$  signal was taken into account by the method of Santrock *et al.* (Santrock *et al.* 1985)

The steroids analyzed with no modulation were used to calibrate  $\text{CO}_2$  gas, which in turn was used to calculate the  $\delta^{13}\text{C}_{\text{VPDB}}$  of sample analytes. From a freshly filled  $\text{CO}_2$  gas volume, three  $\text{CO}_2$  pulses were admitted near the beginning of each run. The known  $\delta^{13}\text{C}_{\text{VPDB}}$  values (Zhang *et al.* 2008) were assigned to the steroid components in the SAXICAB software to calibrate and calculate an “apparent”  $\delta^{13}\text{C}_{\text{VPDB}}$  for the  $\text{CO}_2$  gas. Then the “apparent”  $\delta^{13}\text{C}_{\text{VPDB}}$  was assigned to the  $\text{CO}_2$  gas in the software. This “apparent”  $\delta^{13}\text{C}_{\text{VPDB}}$  of the  $\text{CO}_2$  gas was hence used to calculate the  $\delta^{13}\text{C}_{\text{VPDB}}$  values for the analytes in the modulated sample runs and again to recalculate the  $\delta^{13}\text{C}_{\text{VPDB}}$  values for the non-modulated sample runs. The  $\text{CO}_2$  gas was calibrated for its apparent  $\delta^{13}\text{C}_{\text{VPDB}}$  against the four steroids  $5\alpha$ -andro-AC, andro-AC, 11-keto-AC, and cholestane. The following procedure was used for the reconstruction of modulated peaks for the calculation of their  $\delta^{13}\text{C}_{\text{VPDB}}$ . A peak start and stop time was chosen for the first modulation of the analyte. The  $\delta^{13}\text{C}_{\text{VPDB}}$  was calculated for the peak slice in this time bin relative to the apparent  $\delta^{13}\text{C}_{\text{VPDB}}$  of  $\text{CO}_2$  gas pulses emitted to the IRMS during the beginning of the GCxGCC-IRMS runs. For each additional peak slice, the modulation frequency (i.e. 4 sec) was added to the start and stop times of the previous slice and used as the following modulation time bin. The  $\delta^{13}\text{C}_{\text{VPDB}}$  was then calculated based on the sum of the signal areas of the current slice and all the previous slices. The same time bins were used for all GCxGCC-IRMS runs in a data set.

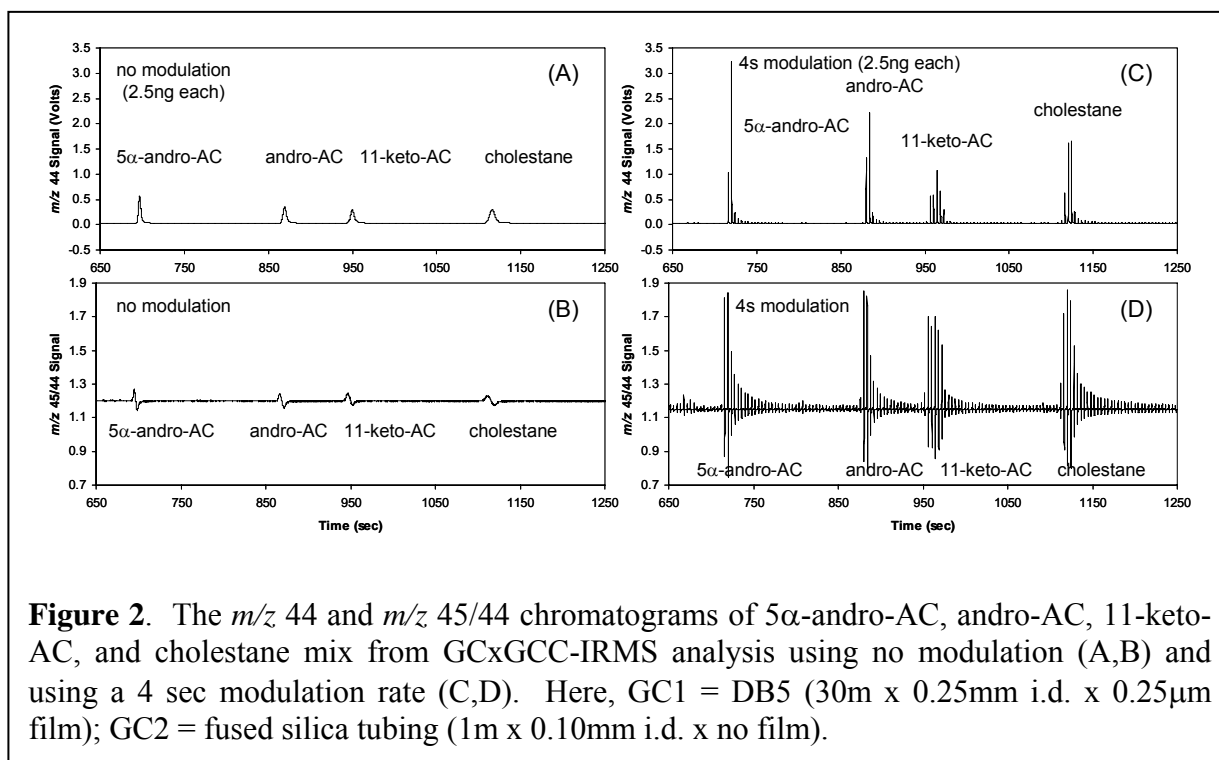
Although the data is seen as a 1D chromatogram in the software, this procedure mimics “boxing” a region for a compound on a 2D contour plot.

### *Results and Discussion*

GCxGC Combustion Interface. Many components of the combustion interface were modified from what is conventionally used for GCC-IRMS in order to improve the minimal obtainable peak width in the system and are further detailed in our work on the development of fast GCC-IRMS (Sacks *et al.* 2007).

Combustion Reactor. Ceramic or quartz tubes that are 0.5 mm i.d. or larger and loaded with CuO, NiO, and Pt wire are typically used in traditional and commercially available GCC-IRMS systems. A single capillary design is better suited to minimization of peak broadening where large i.d. changes and dead volumes can be better controlled, reduced, and at some points eliminated (Goodman 1998). In our fast GCC-IRMS work, we developed a narrow i.d. combustion reactor that enabled ~250 ms FWHM peak widths for the unretained gas CH<sub>4</sub> (Sacks *et al.* 2007). This reactor was composed of a continuous 0.25 mm i.d. fused silica capillary, where the combustion region was loaded with one strand of 0.1 mm diameter Cu wire and oxidized *in situ*.

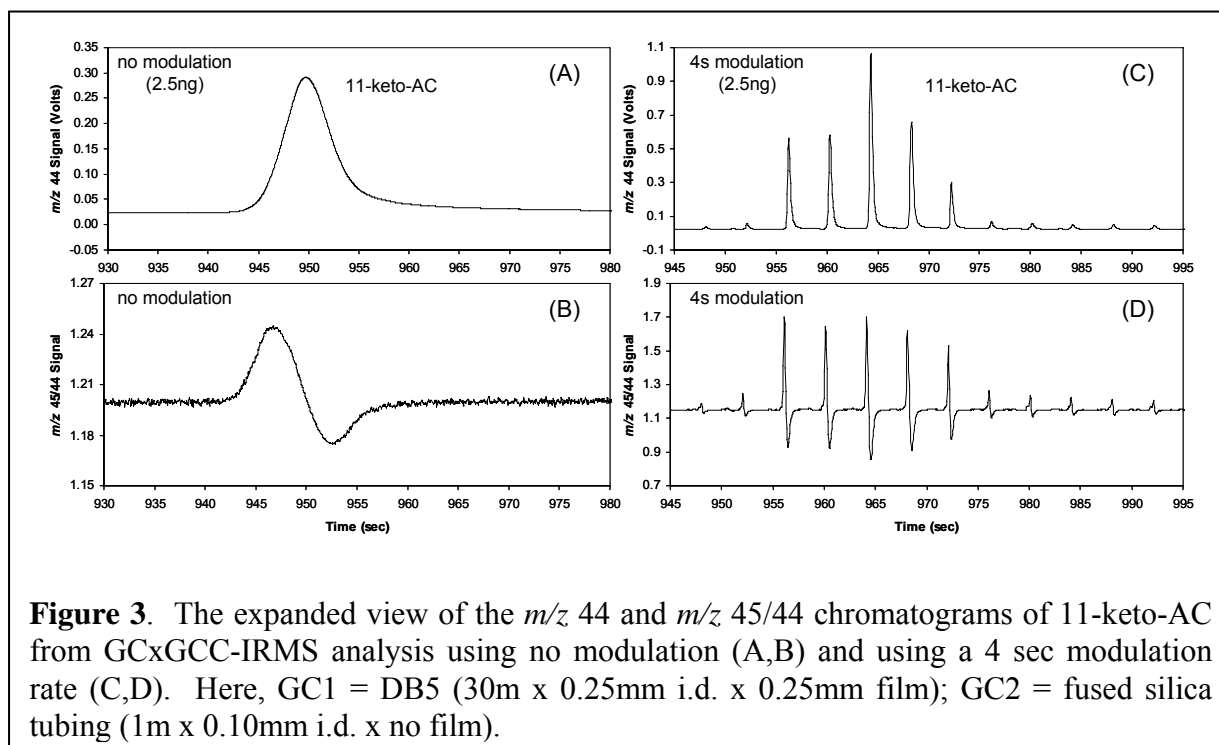
The hand-loading of 0.1 mm Cu (>99% ) wire into a 0.25 mm i.d. capillary can be difficult and cumbersome and is feasible for loading of only a single strand. In this work, we continued to adapt this capillary combustion reactor design, with a qualitative investigation into a small spectrum of other 0.1 mm wire properties. The use of Cu (>99%) wire is problematic for capillary loading due to its softness and high malleability; therefore, it very easily kinks upon handling and loading. On the other hand, Ni (>99%) wire is relatively rigid, but also very springy where it retains its coiled nature from the wire spool. Other wires qualitatively fell between the properties of Cu (>99%) and Ni (>99%) in the following order: Cu (>99%), Cu/Mn/Ni (84/12/4%), Pt (>99%), Cu/Ni (55/45%), and Ni (>99%). While Cu was difficult to load due to kinking, all the other metals were easy to load due to the wires being rigid enough that kinking was not an issue. On the other hand, we speculate there were two issues associated with the more rigid and springy metals such as Cu/Ni (55/45%) and Ni (>99%). These metals often led to capillary cracking upon heating up to 925°C, possibly because they slightly bent/stressed the capillary and/or easily scratched the inside of the capillary during loading, both compromising the integrity of the capillary at high temperatures. We found 0.1 mm Cu/Ni/Mn (84/12/4%) and 0.1 mm Pt (>99%) to have the best properties for



0.25 mm capillary hand-loading and capillary robustness at high temperatures. In addition, we were easily able to load a 0.25 mm i.d. capillary with 2 strands of these wires, which was not possible with Cu (>99%). This allows the construction of a reactor with greater oxidation capacity. These narrow capillary reactors can be very fragile; however, a carefully built and maintained reactor can have a physical lifetime on the order of a month or more.

Modulated and Non-modulated Analysis. Samples analyzed in this study are referred to as “modulated” or “non-modulated”, where all samples were run through the GCxGCC-IRMS system (i.e. through GC1 and GC2) with the LMCS cryogenic modulator, on or off, respectively. The non-modulated analyses are representative of conventional GCC-IRMS analyses and were used to calibrate the CO<sub>2</sub> pulses used in  $\delta^{13}\text{C}_{\text{VPDB}}$  calculation of modulated analytes as discussed in the materials and methods section.

Modulated Peak Shapes. The mixture of the 4 steroids 5 $\alpha$ -andro-AC, andro-AC, 11-keto-AC, and cholestane was analyzed by GCxGCC-IRMS to investigate the characteristics of modulated peaks that elute off of a 1 m GC2 capillary and combustion interface. The non-modulated (Figure 2A) and the 4 sec modulated (Figure 2C)  $m/z$  44 chromatograms of the mixture show the steroids were well separated in GC1. Also shown are the non-modulated (Figure 2B) and the 4 sec modulated (Figure 2D)  $m/z$  45/44 isotope ratio traces of the mix. All signals are shown at the same scale for comparison. In both cases, 2.5ng of each compound was analyzed and a large increase in signal intensity can be seen for the modulated analytes



over the non-modulated analytes. When not modulated, these steroids had  $m/z$  44 FWHM peak widths increase over a very large range (2866-6777 ms) as compound GC1 retention times increased (720-1130 sec). However, when modulated at 4 sec intervals, the FWHM sliced peak widths of these steroids fall in the range of 288-384 ms, with an average of  $328 \text{ ms} \pm 8\%$ . These sliced peak widths are within the realm required for GCxGC. An expanded view of non-modulated (Figure 3A) and 4 sec modulated (Figure 3C)  $m/z$  44 chromatograms of 11-keto-AC demonstrates baseline separation between the peak slices generated from the modulation. In addition, an expanded view of non-modulated (Figure 3B) and 4 sec modulated (Figure 3D)  $m/z$  45/44 isotope ratio trace of 11-keto-AC depict the well known effect of  $^{13}\text{C}$  enrichment at the peak front to  $^{13}\text{C}$  depletion at the peak end, relative to background. The  $m/z$  45/44 isotope ratio trace in Figure 4D also demonstrates baseline separation between the peak slices.

Quantitative Analysis. Quantitative carbon isotopic composition reconstruction of cryogenically sliced GC1 peaks due to modulation was evaluated. The CIR values were calculated for both the non-modulated and modulated analyses according to the routine described in the material and methods section. For the modulated analysis, results for consecutively summed peak slices are plotted in Figure 4. It can be seen that the earlier peak slices are highly enriched and are associated with large errors. As more peak slices are summed, the CIR values rapidly decrease, which is expected from the isotope ratio trace, and



Component	Calibrated $\delta^{13}\text{C}_{\text{VPDB}}$ (‰)	No Modulation (10ng; n=5)				4s Modulation (2.5ng; n=6)				
		$\delta^{13}\text{C}_{\text{VPDB}}$ (‰)	SD (± ‰)	95% Conf. (± ‰)	Accuracy (‰)	$\delta^{13}\text{C}_{\text{VPDB}}$ (‰)	SD (± ‰)	95% Conf. (± ‰)	Accuracy (‰)	Slices (#)
5 $\alpha$ -andro-AC	-30.61	-30.34	0.29	0.24	-0.27	-30.09	0.36	0.28	0.52	4-6
andro-AC	-33.04	-31.70	0.23	0.20	1.33	-32.32	1.23	0.98	0.72	4-6
11-keto-AC	-16.70	-16.29	0.34	0.29	0.40	-16.49	0.35	0.28	0.21	7-9
cholestane	-24.77	-24.83	0.38	0.34	-0.07	-24.58	0.56	0.45	0.19	6-8

**Table 1.** Comparison of the quantitative carbon isotopic analysis of 5 $\alpha$ -andro-AC, andro-AC, 11-keto-AC, and cholestane by the GCxGCC-IRMS system using no modulation and using a 4 sec modulation rate with peak slice reconstruction.

the magnitude of the errors diminish. A determination on which is the final peak slice for each analyte in this data set is not immediately obvious due to some tailing in the GC1 peak, where the end of the peak slices is difficult to distinguish from column bleed. Nevertheless, the CIR values ultimately plateau in the last three peak slice sums for each analyte, signifying the end of the analyte peak. The final numerical results are presented in Table 1, where the average of the last three peak slice sums are used as the reconstructed CIR values. The modulated and non-modulated analyses result in similar

$\delta^{13}\text{C}_{\text{VPDB}}$  values, where the integration of sliced peaks produced CIR values with average standard deviations of 0.6 ‰ and accuracies within 0.4 ‰. These findings indicate the feasibility of using GCxGC separations with on-line C-IRMS.

**Future work.** Further optimization of the GCxGCC-IRMS system will involve installation of a Programmed Temperature Vaporization (PTV) inlet (Flenker *et al.* 2007) in which solvent can be vented from a cooled inlet prior to sample transfer to GC1. This will help sharpen GC1 analyte peaks upon injection, since split/splitless inlets are susceptible to solvent induced peak broadening. The PTV will also obviate the use of a rotary valve for solvent diversion, which

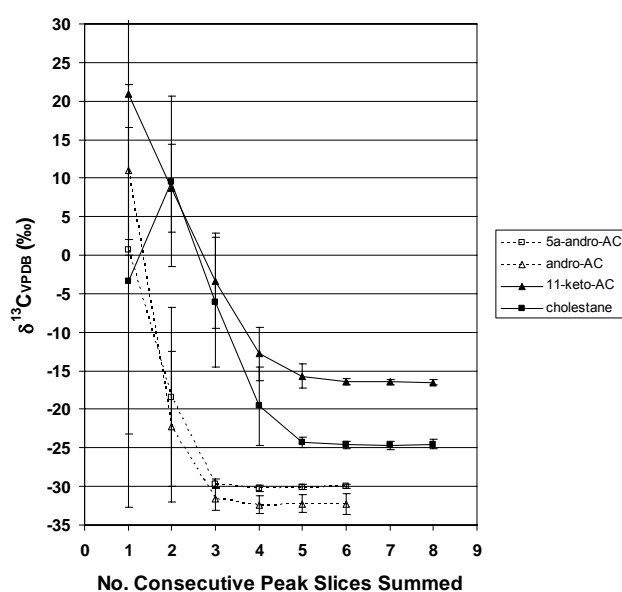


**Figure 4.** Dependence of the number of consecutively summed peak slices of 5 $\alpha$ -andro-AC, andro-AC, 11-keto-AC, and cholestane due to 4 sec modulation in GCxGCC-IRMS on the absolute  $\delta^{13}\text{C}_{\text{VPDB}}$ .

will additionally reduce any peak broadening and tailing in GC1 due to connections, dead volumes, and diameter changes associated with the rotary valve. This modification should improve definition of initial and final peak slices for modulated analytes. Moreover, we will pursue CIR reconstruction of sliced peaks separated in GC2.

### *Acknowledgements*

This work was supported by the United States Anti-Doping Agency, Colorado Springs, CO.

### *References*

Aguilera, R., Catlin, D. H., Becchi, M., Phillips, A., Wang, C., Swerdloff, R. S., Pope, H. G., and Hatton, C. K. (1999). Screening urine for exogenous testosterone by isotope ratio mass spectrometric analysis of one pregnanediol and two androstane diols. *J. Chromatogr. B. Biomed. Sci. Appl.* **727**, 95-105.

Asche, S., Michaud, A. L., and Brenna, J. T. (2003). Sourcing organic compounds based on natural isotopic variations measured by high precision isotope ratio mass spectrometry. *Curr. Org. Chem.* **7**, 1527-1543.

Flenker, U., Hebestreit, M., Piper, T., Hulsemann, F., and Schanzer, W. (2007). Improved performance and maintenance in gas chromatography/isotope ratio mass spectrometry by precolumn solvent removal. *Anal. Chem.* **79**, 4162-4168.

Goodman, K. J. (1998). Hardware Modifications to an Isotope Ratio Mass Spectrometer Continuous-Flow Interface Yielding Improved Signal, Resolution, and Maintenance. *Anal. Chem.* **70**, 833-837.

Liu, Z., and Phillips, J. B. (1991). Comprehensive Two-Dimensional Gas Chromatography using an On-Column Thermal Modulator Interface. *J. Chromatogr. Sci.* **29**, 227-231.

Marriott, P. J., and Kinghorn, R. M. (1997). Longitudinally modulated cryogenic system. A generally applicable approach to solute trapping and mobilization in gas chromatography. *Anal. Chem.* **69**, 2582-2588.

Mondello, L., Tranchida, P. Q., Dugo, P., and Dugo, G. (2008). Comprehensive two-dimensional gas chromatography-mass spectrometry: A review. *Mass Spectrom. Rev.* **27**, 101-124.

Sacks, G. L., Zhang, Y., and Brenna, J. T. (2007). Fast Gas Chromatography Combustion Isotope Ratio Mass Spectrometry. *Anal. Chem.* **79**, 6348-6358.

Santrock, J., Studley, S. A., and Hayes, J. M. (1985). Isotopic Analyses Based on the Mass-Spectrum of Carbon-Dioxide. *Anal. Chem.* **57**, 1444-1448.

Zhang, Y., Tobias, H. J., and Brenna, J. T. (2008). *Steroids*, submitted for publication.